Nuclear-Structure Studies in the Nickel Isotopes with (d,t) Reactions*

R. H. FULMER† AND W. W. DAEHNICK
University of Pittsburgh, Pittsburgh, Pennsylvania
(Received 22 March 1965)

Nuclear levels of the nickel isotopes were investigated with (d,t) reactions at 15-MeV deuteron energy. Absolute differential cross sections were obtained from isotopically enriched Ni^{58}, Ni^{60}, Ni^{61}, Ni^{62}, and Ni^{64} targets with ΔE-$\times$-E counter telescope and two-parameter multichannel analysis. Two sets of distorted-wave Born approximation (DWBA) calculations were made for all Q values and l values of interest, and spectroscopic factors and l values were extracted from the comparison of data and theory. In addition, a number of j values, for the final states, were assigned on the basis of empirical rules. A j dependence was observed for all $l=1$ and $l=3$ transitions where resolution and statistics were good enough to allow analysis of the data for angles larger than about 45°. For all but the very weakly excited levels, correct j values could also be obtained from a comparison of (d,p) and (d,t) spectroscopic factors leading to the same final state. It was noted that a number of $l=3$ transitions previously observed by Cohen, Fulmer, and McCarthy in Ni(d,p) reactions led to final states that we find to be $f_{7/2}$. This indicates that in the light Ni isotopes the $f_{7/2}$ shell is not completely filled. The spectroscopic factors reported are discussed in terms of the shell-model pairing theory by Kisslinger and Sorensen. Our results for the energies and fullness of single-quasiparticle levels are in agreement with results from (d,p) work provided the correct j assignments are used. It was found that all DWBA predictions without $\mathbf{l}\cdot\mathbf{s}$ interaction failed to give good quantitative agreement with the observed (d,t) angular distributions for angles beyond the stripping peak. DWBA calculations were made for a conventional neutron form factor which is determined by the neutron separation energy, and also for a recently suggested form factor which is determined by a constant binding energy for all neutrons with a given j, regardless of differences in separation energy. The two form factors lead to almost identical predictions for the angular distributions; however, systematic differences are found in the spectroscopic factors. In terms of shell-model expectations, the conventional approximation for the neutron form factor leads to more consistent results.

I. INTRODUCTION

SINGLE-NUCLEON stripping and pick up reactions such as (d,p), (He^3,d), (p,d), (d,t), etc., predominantly lead to final states which have appreciable single-particle components. To the large extent that the theory of direct interactions is applicable, such reactions have provided much nuclear-structure information. They have been employed extensively, not only to measure angular momentum and parity of the final states, but also to find experimentally the energies of "single-particle" levels (by stripping on targets with doubly closed shells). More recently,[1,2] stripping reactions on nuclei with only one closed shell (usually protons) have been used to arrive at single-quasiparticle energies. Here it is necessary to observe all levels into which the single-particle levels are split by residual interactions. The single-quasiparticle energies, of course, are not observed directly, but are usually computed from the "center of gravity" of the actually observed levels of given orbital and total angular momentum. Cohen[1] defines the "center of gravity" E_j of a group of states as

$$E_j=\sum_i S_i E_j^i/\sum_i S_i. \quad (1)$$

This means a weighted average over the energies of all observed levels with l, $j=$const is computed. The weighting factors S_i are the spectroscopic factors obtained from a comparison of distorted-wave Born approximation calculations (DWBA) with experimental cross sections. This provides us with a precise and justifiable definition of experimental single (quasi)-particle energies E_j. For the case of one nucleon outside doubly closed shells, of course, E_j becomes identical to the single-particle energy.

The present work was designed to complement earlier work with (d,p) reactions[2] and (d,t) reactions[3] on Ni isotopes, particularly to help in the assignment of uncertain spins, and in the investigation of the Ni^{57} nucleus, which cannot be investigated with stripping reactions. The levels of Ni^{57} are important from the standpoint of the shell model, since Ni^{57} has a single neutron outside a doubly magic core of 28 neutrons and 28 protons. For the other nickel isotopes, (d,t) cross sections for levels of known spin can be used to check the rule that the total angular momentum of a level is indicated by the ratio of stripping to pickup cross sections which lead to the same final state. It was also desired to compare the spectroscopic information obtained from (d,p) work with that from (d,t) experiments. If the DWBA theory is fully applicable, (d,p) and (d,t) are complementary reactions and should lead to the same values for the fullness of certain final states and for the quasiparticle energies. The precise values for these quantities depend critically on the spectroscopic factors S_i which in turn are sensitive to certain approxi-

* Work supported by the National Science Foundation under Grant No. G-11309.
† Present address: Knolls Atomic Power Laboratory, General Electric Company, Schenectady, New York.
[1] B. L. Cohen, R. H. Fulmer, and A. L. McCarthy, Phys. Rev. **126**, 698 (1962).
[2] R. H. Fulmer and A. L. McCarthy, Phys. Rev. **131**, 2133 (1963); R. H. Fulmer, A. L. McCarthy, B. L. Cohen, and R. Middleton, *ibid.* **133**, B955 (1964).
[3] M. H. MacFarlane, B. J. Raz, J. L. Yntema, and B. Zeidman, Phys. Rev. **127**, 204 (1962).

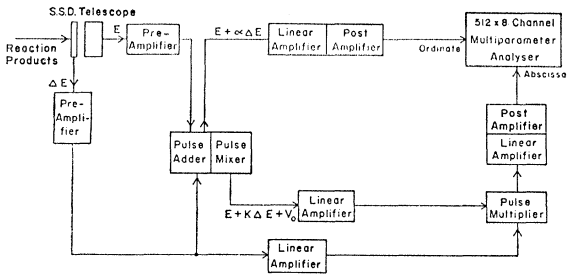

FIG. 1. Block diagram of the counter-telescope electronics used to study (d,t) reactions.

mations made in DWBA calculations. Traditionally, the neutron form factor is computed from the actual separation energy of the picked-up neutron, but more recently possible improvements have been discussed.[4,5] One of the simpler new recipes suggests that the energy for a neutron in the proper "single-particle" state should be used.[4] Some calculations using either approach were made. The results will be compared with each other and with experimental data, with the intent to arrive at an opinion on the reliability of spectroscopic factors obtained in our work. Acutally, theoretical ambiguities are only part of the problem. Experimental limitations, in particular for highly excited levels, may be quite severe, and will be discussed below.

II. EXPERIMENTAL PROCEDURE

A factor that contributes strongly to experimental problems in (d,t) work is the fact that Q values are always negative. They range from -3 to -7 MeV for ground-state transitions, and are still more negative for transitions to excited states. Hence, deuteron-induced reactions yield protons, deuterons, and α particles of energies higher than that of the most energetic tritons, and the selection of tritons is not trivial. In the special case of small negative Q values, one-parameter magnetic analysis of tritons remains possible. If the most energetic deuterons are of 15 MeV they will coincide, in the focal plane of an analyzing magnet, with triton groups of about 10 MeV. Tritons of higher energies have enough magnetic rigidity to be resolved from all deuterons, protons and alphas that can be produced in experiments with 15-MeV deuterons. Magnetic analysis has been used for some previous work on (d,t) reactions,[6,7] and also for some of the data presented in this paper. Generally, however, the tritons of interest in the investigation reported here had energies below 10 MeV, and had to be identified by two-parameter analysis. The parameters measured were the total particle energy E and the energy loss ΔE in a thin transmission counter. As is well known,[8] the product $\Delta E(E'+\frac{1}{2}\Delta E+V_0)=P(m,z)$ is approximately constant for particles of like mass if $\Delta E \ll E'$. Hence if $E=E'+\Delta E$ is fed into the Y input and the product $P(m,z)$ into the X input of a 2-dimensional analyzer (Nuclear Data 160 FM) all counts will cluster around parallel lines, $P(m,z)\sim mz^2$, which are distinguished by a certain mass and charge combination. A block diagram of our electronic apparatus is shown in Fig. 1.

In the past, the pulses $P(m,z)$ were usually fed into a single-channel analyzer set for the correct value, in order to gate a one-dimensional analyzer with the discriminator output. The latter method is very convenient if $P(m,z)$ is really very close to constant, or if the energy range of interest is small compared to the triton energies. In our experiment neither condition was fulfilled. The tritons analyzed had energies from 6–12 MeV, and $P(m,z)$ was not quite constant near the lower energy limit, so that the two-dimensional display was essential for unambiguous particle selection. A second advantage in the use of a two-dimensional analyzer is the possibility of simultaneously measuring inelastic deuteron scattering events. Such measurements were made in a few experiments.[9] The separation of deuterons from tritons by the $\Delta E \times E''$ method is generally good although not ideal. With the use of surface-barrier counters, the energy resolution in both counters can be quite good, i.e., 20 keV or better for

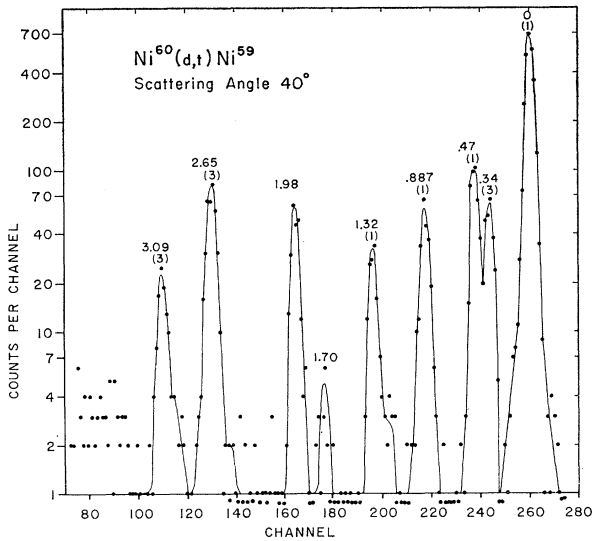

FIG. 2. Measured triton energy spectrum from $Ni^{60}(d,t)Ni^{59}$. Numbers above peaks are excitation energies in Ni^{59} in MeV, and l values assigned to the peaks are in parentheses. Energy resolution here is typical of the experiment. Points below one indicate zero counts.

[4] E. Rost, B. F. Bayman, and R. Sherr, Bull. Am. Phys. Soc. **9**, 458 (1964); and E. Rost (to be published).
[5] N. Austern, Phys. Rev. **136**, B1743 (1964); W. T. Pinkston and G. R. Satchler (to be published).
[6] B. L. Cohen and R. E. Price, Phys. Rev. **121**, 1441 (1961).
[7] R. H. Fulmer, A. L. McCarthy, and B. L. Cohen, Phys. Rev. **128**, 1302 (1962).
[8] H. A. Bethe, *Handbuch der Physik*, XXIV, edited by H. Geiger and K. Scheel (Julius Springer-Verlag, Berlin, 1933), 2nd ed., p. 518.
[9] R. K. Jolly, Ph.D. thesis, University of Pittsburgh (unpublished).

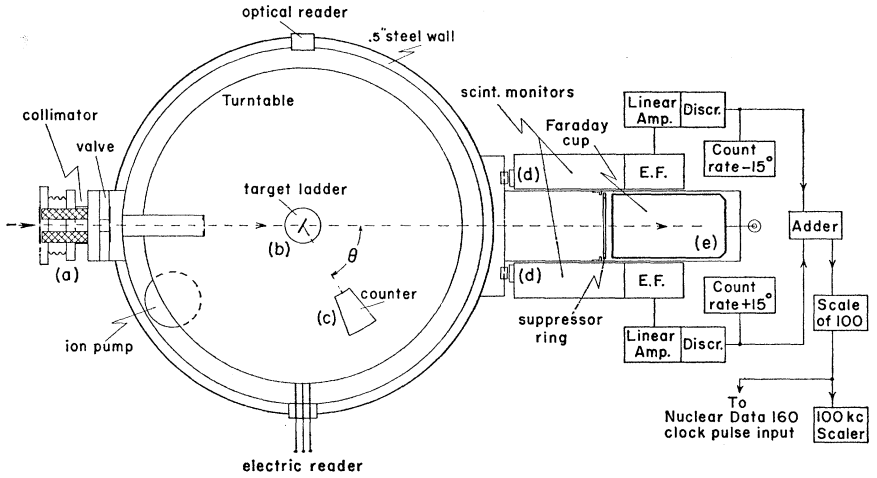

FIG. 3. Schematic view of scattering chamber and monitoring system. Beam enters chamber through collimating slits near (a) and impinges on target at (b). The detector, at (c), is mounted on a turntable (inmost circle). Scintillation detectors at (d) monitor the scattered beam; the unscattered beam is collected in a Faraday cage at (e).

6–10-MeV particles. This would lead to a relatively small spread in the value of P and would not hinder particle separation. However, the energy deposited by a transient particle in the first (ΔE) counter of a counter telescope is subject to straggling. Usually the variation of ΔE due to straggling was much larger than the uncertainty in the ΔE measurement due to finite resolution caused by detector noise. If good particle resolution is desired, it is advantageous to make the ΔE counter fairly thick so that the straggling width becomes small with respect to $(\Delta E)_{\text{av}}$. For this experiment we chose a ΔE counter of about 60 μ as a reasonable compromise. This counter stopped 3.5-MeV tritons. $\Delta E \times E''$ analysis was possible for $\geq$6-MeV tritons, i.e., for Q values down to -9 MeV. The E counter was a 1-mm-deep gold surface-barrier detector and completely stopped all deuterons and tritons. A simple home-built mixing circuit provided the signals $E'+\Delta E=E_{\text{total}}$ for the multichannel analyzer, and the signal $E''=E'+k\Delta E+V_0$ for one of the multiplier inputs. k and V_0 were variable and were adjusted to make the product $P=\Delta E \times E''$ most nearly constant in the region of interest. The multiplication module consisted of two logarithmic attenuators[10] with a low-input impedance amplifier, and provided an output very closely proportional to $\log(\Delta E \times E'')$ for input signals from 2 to 100 V. This output was amplified by a post amplifier and fed into the X side of the two-dimensional multichannel analyzer, while the $E'+\Delta E$ signal was fed into the Y input. Amplifier biases and gains were set so as to spread the deuteron and triton ridges over about 8 channels. The selected energy interval included 6–15 MeV, and was analyzed into 512 channels (see Fig. 1).

The counter telescope set up in this way provided good particle and energy resolution. Figure 2 shows a typical (d,t) spectrum which was obtained by summing over the four $\log(\Delta E \times E'')$ channels that corresponded to triton counts. While the detectors and the analyzer individually were capable of 20-keV resolution, the over-all experimental resolution was rarely better than 70 keV (see Fig. 2). This value is explained as the random sum of finite resolution in detectors, analyzer, and beam energy plus straggling in the target, kinematic energy spread due to the finite solid angle, and an apparently strong counting-rate effect. The latter effect and the thickness of our targets (0.5–3.1 mg/cm^2) were the most important factors that limited the over-all energy resolution, which for the thinner targets ranged from 60 keV at small angles to 80 keV at back angles. The Ni^{61} and Ni^{62} targets were, respectively, 3.1 and 1.9 mg/cm^2 thick and could not be used for back-angle measurements. Ni^{58}, Ni^{60}, and Ni^{62} had an isotopic enrichment of better than 99%. Ni^{61} was available only with 83% isotopic enrichment.

All (d,t) counter experiments were performed in our new remotely controlled 18-in.-diam scattering chamber. The chamber is positioned behind a magnetic beam analyzing system that can deliver clean deuteron beams with an energy spread of down to 10 keV in 15 MeV. For the present experiment a beam width of 30 keV was considered adequate. A lead-shielded entrance collimator (Fig. 3) consisting of two 2-mm slits plus anti-scattering slit limits the beam divergence and its deviation from $\theta=0$ to less than $\pm 2°$. Two NaI scintillation counters are permanently mounted at $\pm 15°$ for monitoring purposes. The sum of their elastic deuteron counts monitors beam charge times target thickness. The difference of their counting rates provides an error signal for the true beam zero position. The entire chamber can be rotated around its entrance aperture by remote control, so that $\theta=0$ for the beam direction can easily be found and maintained.

The counter telescope is mounted on a turntable inside the scattering chamber. Its position can be changed continuously from $\theta=0$ to $\pm 170°$ by remote control. The turntable position is marked in 1° intervals, and visual readings for θ can be taken to an accuracy of $\pm 0.1°$. A remote (electric) reader is calibrated in 5°

[10] C. H. Vincent and D. Kaine, IRE Trans. Nucl. Sci. NS-9, 327 (1962).

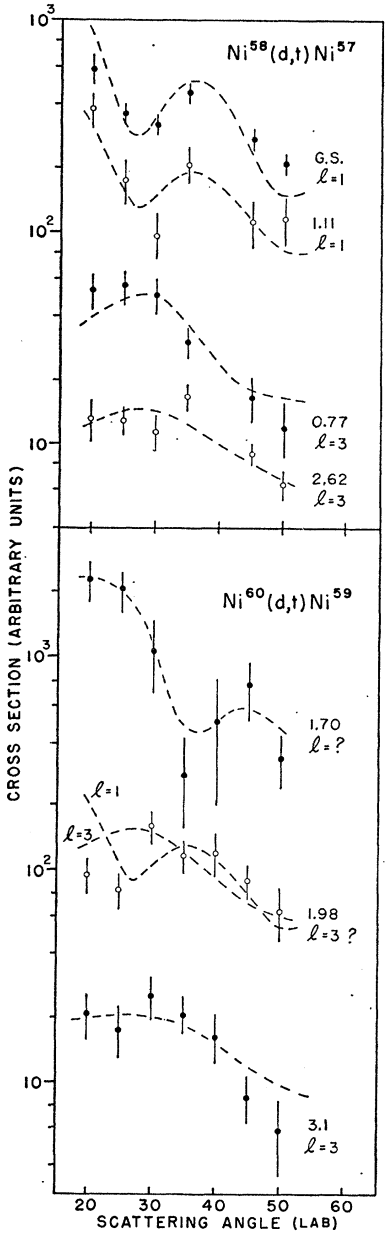

FIG. 4. Some angular distributions for levels observed in the reactions $Ni^{58}(d,t)Ni^{57}$ and $Ni^{60}(d,t)Ni^{59}$. The dashed lines are typical DWBA predictions except where l is not indicated. Numbers opposite the curves are excitation energies in MeV.

TABLE I. Results of the $Ni^{58}(d,t)Ni^{57}$ reactions.

(1) Excitation energy (MeV)	(2) l	(3) J	(4) $(d\sigma/d\omega)_{max}$ (mb/sr)	(5) S' SE	(6) S' CB
0	1	$\frac{3}{2}$	0.637	1.05	1.01
0.77	3	$\frac{5}{2}$	0.070	0.69	0.60
1.12	1	$\frac{1}{2}$	0.054	0.23	0.23
2.62	3	$\frac{7}{2}$	~0.10	~2.7	8.7

TABLE II. Results of the $Ni^{60}(d,t)Ni^{59}$ reactions.

(1) Excitation energy (MeV)	(2) l	(3) J	(4) $(d\sigma/d\omega)_{max}$ (mb/sr)	(5) S' SE	(6) S' CB
0	1	$\frac{3}{2}$	1.83	2.22	2.36
0.34	3	$\frac{5}{2}$	0.20	1.15	1.24
0.47	1	$\frac{1}{2}$	0.25	0.41	0.52
0.89	1	$\frac{3}{2}$	0.116	0.25	0.22
1.32	1	$\frac{1}{2}$	0.068	0.22	0.23
1.70	...	...	~0.04	...	...
1.98	(3)	...	0.09	...	...
2.65	3	$\frac{7}{2}$	0.27	5.33	18.2
3.09	3	$(\frac{7}{2})$	~0.09	~2.3	~7.8

intervals to an accuracy of $\pm 0.2°$. Targets are mounted on a target ladder which can hold 4 targets simultaneously. At the present time the target angle α can be changed from $-60°$ to $+60°$ and can be reset to $\pm 2°$ accuracy. The counter telescope normally is cooled to about 0°C by a thermoelectric cooler (Westinghouse WX814-J) which dissipates the heat to the turntable. The beam charge is collected in a 5-in.-deep Faraday cup (made of Ta) which intercepts all particles scattered through $\theta \leq 6°$. An electron suppressor ring is provided and is used for vaccuums better than 10^{-5} Torr. For the present experiment the chamber vacuum was typically 5×10^{-4} Torr, and the use of a suppressor voltage was not advantageous. Pumping of the chamber was provided by the magnet vacuum (via the 2-mm entrance slits) and by a 20–140-liter/sec ion pump,[11] which is directly attached to the scattering chamber. A schematic drawing of scattering chamber and monitoring system is shown in Fig. 3.

In order to minimize systematic counting errors the following procedure was used: (a) The total charge was measured (by a commercial virtual earth integrator, Eldorado Company Cl-110) and compared with the sum of the $\pm 15°$ monitor counts. If the two monitors disagreed by more than 5% the run was rejected. Such disagreements occurred in a few cases and could be traced to either faulty charge integration for very small currents, or to physical obstruction of one of the 15° monitors.

(b) The sum of the 15° monitor counts was fed into a 10-Mc/sec prescaler (Hewlett Packard) which reduced the pulse rate by a factor of 100. The output of this scaler was then used as input for the "clock" channel of our multichannel analyzer. These clock pulses are subject to the same analyzer dead time losses as other counts; and the use of stored clock pulses for normalization automatically eliminates errors due to dead time losses as well as errors due to the uncertainty in the target angle and target nonuniformity.

[11] ULTEC Boostivac. This pump unfortunately did not perform according to specifications and proved of little or no use during the time this experiment was performed. Therefore, the absolute-cross-section calibration for this experiment was obtained by normalization of the telescope data to some runs that employed magnetic analysis.

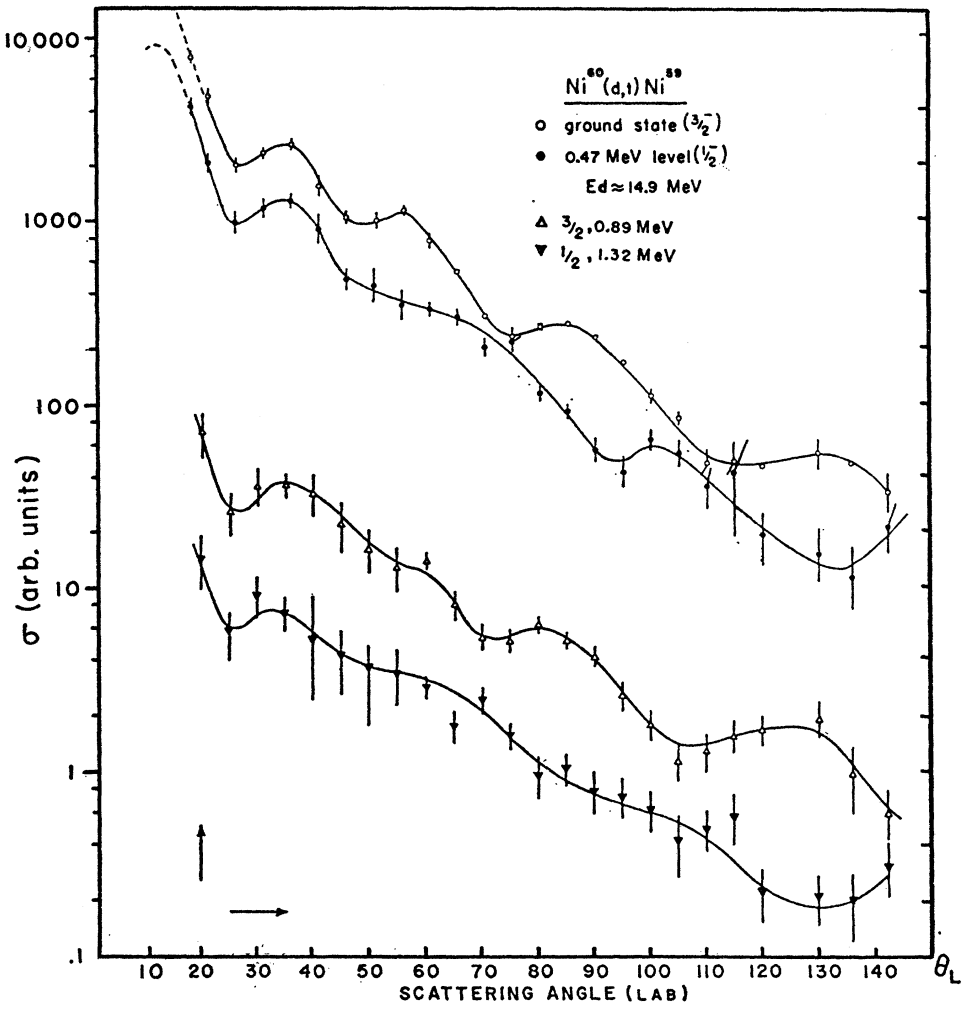

FIG. 5. Comparison of $p_{3/2}$ and $p_{1/2}$ angular distributions for $Ni^{60}(d,t)Ni^{59}$ reactions. Note the differences at large scattering angles. The solid lines are smooth curves drawn through the experimental points to aid the eye. All curves are nearly identical for angles below 40°.

TABLE III. Results of the $Ni^{62}(d,t)Ni^{61}$ reactions.

(1) Excitation energy (MeV)	(2) l	(3) J	(4) $(d\sigma/d\omega)_{max}$ (mb/sr)	(5) S' SE	(6) S' CB
0	1	$\frac{3}{2}$	3.48	2.77	3.72
0.07	3	$\frac{5}{2}$	0.78	2.59	3.72
0.29	1	$\frac{1}{2}$	0.94	0.88	1.40
0.65	1	$\frac{1}{2}$	0.16	0.18	0.26
1.11	1	$(\frac{3}{2})$	0.17	0.26	0.24
1.17	1	$\frac{3}{2}$	0.22	0.34	0.33
1.45	3	$(\frac{7}{2})$	0.16	1.05	4.56
1.61	...	...	~0.068	...	...
1.73	1	$\frac{1}{2}$	0.036	0.08	0.10
2.00	3	$\frac{7}{2}$	~0.027	~0.25	~0.96
2.14	$\binom{1}{+4}$	$\binom{\frac{1}{2}}{+\frac{9}{2}}$	~0.023 ~0.03	~0.08 ~0.72	~0.08 1.32
2.48	...	...	~0.048	...	...
2.92	3	$\frac{7}{2}$	0.11	1.58	5.79
3.13	...	...	~0.049	...	...
3.31	3	$\frac{7}{2}$	0.12	2.08	7.32
3.63	3	$\frac{7}{2}$	~0.034	~0.76	~2.55

III. EXPERIMENTAL ERRORS

Our largest experimental errors are scale errors which affect all points of a given angular distribution in the same way. They are almost exclusively caused by two factors: (a) an uncertainty in the target thickness of about ±10%, and (b) the error in the absolute calibration of the charge integration, which we also estimate at about 10%. These systematic errors could cancel as well as add, and we assign a probable scale error of ±15%. Scale errors are not shown in our figures and tables. In addition to scale errors in the cross section we have systematic errors introduced by uncertainties in the scattering angle θ. The angular resolution was about $\Delta\theta = 1.5°$. The uncertainty in the zero position was less than ±1°.

Random errors differ widely from point to point. They are due to statistics, background subtraction, limited energy resolution and the resultant difficulty in resolving nearby peaks. Random errors are estimated for each point and shown in the figures.

The excitation energies quoted for various levels are

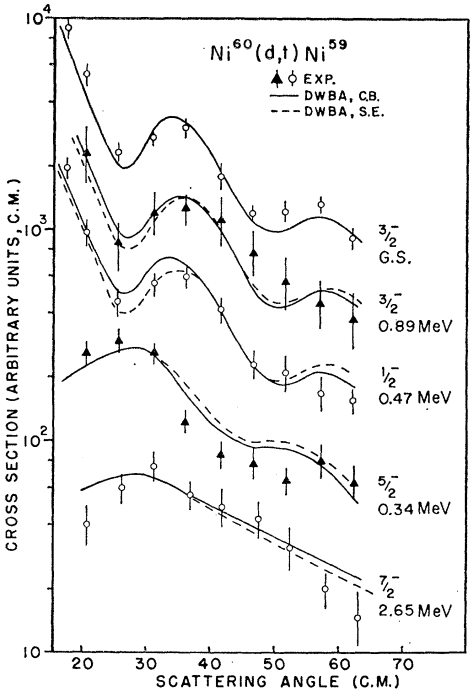

FIG. 6. Comparison of experimental angular distributions with different DWBA predictions for the $Ni^{60}(d,t)Ni^{59}$ reactions. Numbers opposite the curves give J, parity, and the excitation energy of the level. The symbols CB and SE are explained in the text (G.S. = ground state).

uncertain to about 10–30 keV, depending on energy resolution and the proximity of a well-known peak for which the energy could be taken from the literature.

IV. ASSIGNMENT OF l AND J

A. Assignments of Orbital-Angular-Momentum Values

Angular distributions for levels observed in the (d,t) reactions are shown in Figs. 4–10. The l-transfer assignments for levels of Ni^{57}, Ni^{59}, Ni^{61}, and Ni^{63} are listed in column (2) of Tables I–IV, respectively. The assignments of orbital angular momenta from the (d,t) angular distributions are in very good agreement with similar assignments from (d,p) reactions.[2]

Theoretical predictions for the $Ni^{60}(d,t)Ni^{59}$ angular distributions were obtained by DWBA calculations; representative curves are shown in Figs. 4, 6, 7, 8, and 9. The optical-model parameters used in the calculations are listed in Table V. No spin-orbit terms were included in the optical-model potentials. Since triton parameters were not available in the nickel region, parameters for the DWBA calculations were based on the available analysis of He^3 elastic-scattering data.[12] Three reasonable sets of parameters were tried; each set predicted essentially the same Q dependence and similar absolute magnitudes for the cross section. For each of these calculations, the binding energy of the transferred neutron was taken as the separation energy of the nuclear level formed in the reaction. The neutron potential was a Wood-Saxon well with a radius parameter of 1.25 F and a diffusivity of 0.65 F. As was noted in the introduction, it was suggested recently that in the distorted-wave calculation of the neutron form factor, one should use

TABLE IV. Results of the $Ni^{64}(d,t)Ni^{63}$ reactions.

(1) Excitation energy (MeV)	(2) l	(3) J	(4) $(d\sigma/d\omega)_{max}$ (mb/sr)	(5) S' SE	(6) CB
0	1	$\frac{1}{2}$	0.87	0.47	1.16
0.09	3	$\frac{5}{2}$	1.65	3.43	6.69
0.16	1	$\frac{3}{2}$	4.26	2.42	4.24
0.53	1	$\frac{3}{2}$	1.23	0.82	1.25
1.01	1	$\frac{1}{2}$	0.64	0.52	0.91
1.27	$\binom{1}{+4}$	$\binom{\frac{1}{2}}{+\frac{9}{2}}$	0.19	~0.09 ~0.82	~0.15 ~1.98
1.77	3	$\frac{7}{2}$	~0.049	~0.23	~1.17
1.91	3	$\frac{7}{2}$	0.087	0.45	2.19
2.14	1	$\frac{1}{2}$	0.24	0.36	0.47
2.29	...	...	1.10	...	...
2.52	(4)	$(\frac{9}{2})$	~0.014	~0.21	0.42
2.98	...	...	0.038	...	...
3.58	(3)	$(\frac{7}{2})$	0.20	2.32	8.88

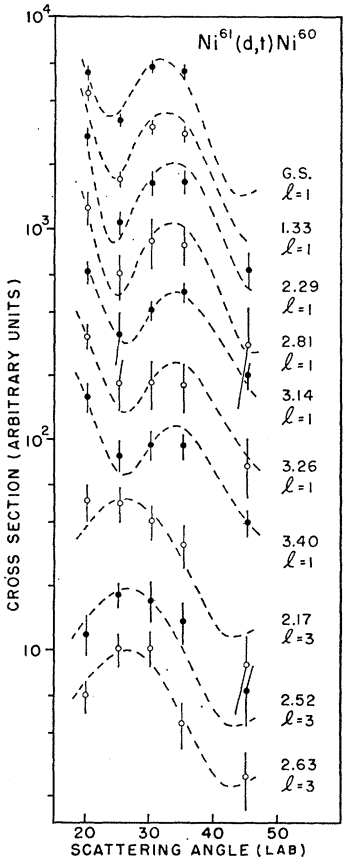

FIG. 7. Angular distributions for levels observed in the reactions $Ni^{61}(d,t)Ni^{60}$. The dashed lines are typical DWBA predictions for the indicated l value. Numbers opposite the curves are excitation energies in MeV.

[12] We are indebted to R. Bassel and R. Drisko for sending us the preliminary parameters for Ni (He^3, He^3)Ni data by Yntema and Zeidman.

TABLE V. DWBA parameters for Ni(d,t) reactions.

Case	V (MeV)	W (MeV)	r_0(F)	r_c(F)	a(F)	r_0'(F)	A'(F)	W'(MeV)
deuteron	79.5[a]	0	1.274	1.3	0.739	1.389	0.625	82[b]
triton A	98[a]	19[a]	1.07	1.4	0.854	1.7	0.75	0
triton B	92[a]	10[a]	1.07	1.4	0.854	1.8	0.592	0
triton C	43[a]	14[a]	1.52	1.4	0.61	...	...	...

[a] Saxon-type well. [b] Surface-absorption-type well.

the binding energy of the single-particle state to which the transferred neutron belongs, independent of the separation energy of the nuclear level formed in the reaction.[4] Such a "constant binding energy" (CB) DWBA calculation was performed with the first set of triton parameters in Table V. Binding energies of the single-particle states were taken from Table VII with an $f_{7/2}-f_{5/2}$ splitting of 6 MeV. The differences in the predicted angular distributions were found to be quite small at forward angles (see Fig. 6). Both the "constant binding energy" and "separation energy" (SE) DWBA calculations agree almost equally well with the experimental angular distributions. In fact, our use of an integration cutoff had a somewhat greater effect on the agreement of DWBA curves with experimental angular distributions than the method of calculating the neutron

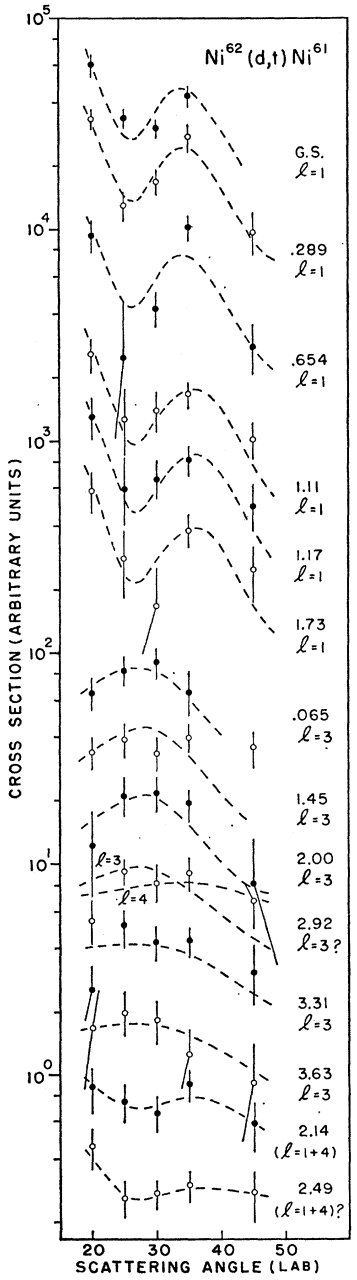

FIG. 8. Angular distributions for levels observed in the reactions Ni$^{62}(d,t)$Ni^{61}. The dashed lines are typical DWBA predictions for the indicated l value. Numbers opposite the curves are excitation energies in MeV.

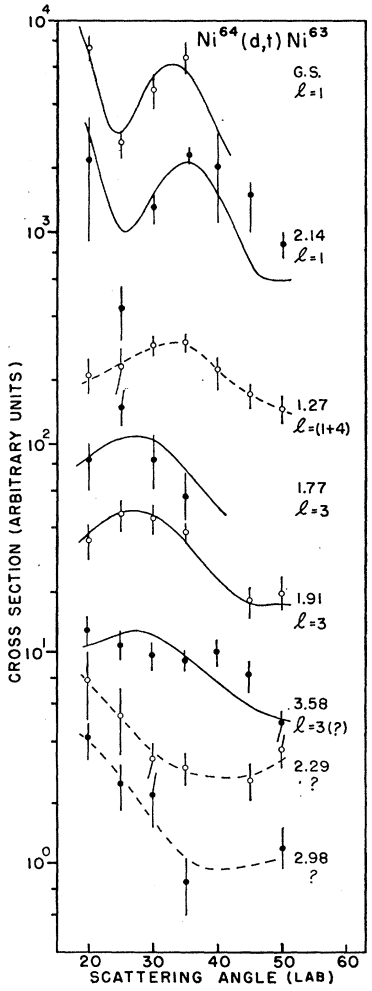

FIG. 9. Some angular distributions for levels observed in the reactions Ni$^{64}(d,t)$Ni^{63}. The dashed lines are smooth curves drawn through the experimental points to aid the eye. Numbers opposite the curves are excitation energies in MeV. Solid lines are DWBA predictions.

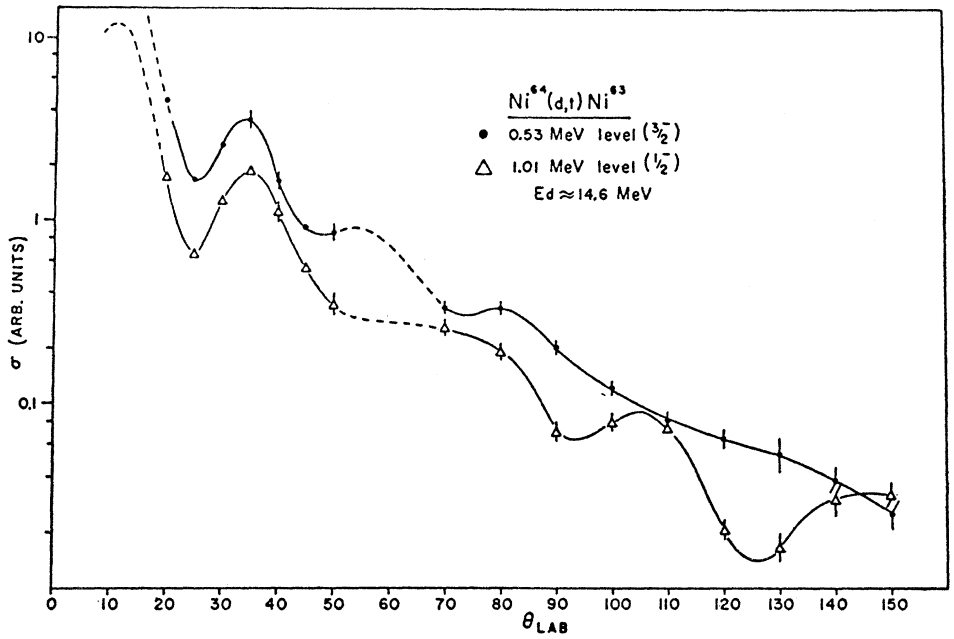

FIG. 10. Comparison of $p_{3/2}$ and $p_{1/2}$ angular distributions for $Ni^{64}(d,t)Ni^{63}$ reactions. Note the differences at large scattering angles.

form factor. Best over-all agreement was obtained with a cutoff at 5.5 F, and this cutoff was used for the computations leading to the spectroscopic factors given in this paper. Other cutoffs near the nuclear surface gave predictions that differed by up to 10% while no cutoff generally led to about 20% larger cross sections. The comparisons of data with the two sets of calculations (Fig. 6) are confined to forward angles, since spin-orbit effects, which were neglected, will influence the predicted angular distributions at large scattering angles. It is remarkable that the predicted angular distributions are so similar for the two approaches, since they do yield widely varying spectroscopic factors for some levels.

B. Assignment of Total Angular-Momentum Values

As Tables I–IV indicate, the orbital angular momenta of levels observed by (d,t) reactions on the nickel isotopes are mostly $l=1$ or $l=3$. Thus the levels may be assigned values of total angular momentum $J=\frac{1}{2}$ or $\frac{3}{2}$, or $J=\frac{5}{2}$, or $\frac{7}{2}$, respectively. The (d,t) reactions provide two indications of the true values of J for the observed levels.

The first indication is found from the angular distributions. For the p levels in the nickel isotopes, the (d,t) angular distributions are strongly J-dependent at large scattering angles, as was reported in Ref. 13. Some of the data of Ref. 13 are shown, with more complete angular distributions, in Figs. 5 and 10. It can be seen that differences in the $J=\frac{3}{2}$ and $J=\frac{1}{2}$ angular distributions occur at angles as low as 60°, and that differences of a factor of three or more are present near 125°. (d,t) angular distributions also show some J dependence for $l=3$ transitions. A typical difference in the angular distributions for $J=\frac{5}{2}$ and $J=\frac{7}{2}$ is seen near the first maximum, and is well illustrated by the lower curves in Fig. 6. The first maximum of the angular distribution seems to occur at slightly more forward angles in the $f_{5/2}$ case than in the $f_{7/2}$ case, and the $f_{5/2}$ angular distribution drops off from this maximum more abruptly than does the $f_{7/2}$ angular distribution. The effect can be partially explained from the fact that the $f_{5/2}$ state is not as deeply bound as the $f_{7/2}$ state. The kinematics of the reaction favor smaller scattering angles for states which are less strongly bound, and this effect is qualitatively predicted by the DWBA calculations. Such dif-

[13] R. H. Fulmer and W. W. Daehnick, Phys. Rev. Letters **12**, 455 (1964).

TABLE VI. Predictions of spins of p levels by the ratio $S(d,p)/S(d,t)$.

Level (excitation energy in MeV)		$S(d,p)/S(d,t)$	Predicted spin	Known spin
Ni^{59}	0	0.85	$\frac{3}{2}$	$\frac{3}{2}$
	0.47	2.1	$\frac{1}{2}$	$\frac{1}{2}$
	0.89	0.86	$\frac{3}{2}$	$\frac{3}{2}$
	1.31	1.8	$\frac{1}{2}$	$\frac{1}{2}$
Ni^{61}	0	0.41	$\frac{3}{2}$	$\frac{3}{2}$
	0.29	0.94	$\frac{1}{2}$	$\frac{1}{2}$
	0.65	(0.15)	...	...
	1.11	0.49	$\frac{3}{2}$	...
	1.17	0.51	$\frac{3}{2}$	...
	1.73	(0.23)	...	...
Ni^{63}	0	1.1	$\frac{1}{2}$	$\frac{1}{2}$
	0.16	0.30	$\frac{3}{2}$	$\frac{3}{2}$
	0.53	0.26	$\frac{3}{2}$	$\frac{3}{2}$
	1.01	0.87	$\frac{1}{2}$	$\frac{1}{2}$
	2.14	(0.07)	...	...

TABLE VII. Excitation energies of single-quasiparticle states.

(1)	(2a)	(2b)	(3a)	(3b)	(4a)	(4b)	(5a)	(5b)
	Ni^{57}		Ni^{59}		Ni^{61}		Ni^{63}	
State	SE	CB	SE	CB	SE	CB	SE	CB
$p_{3/2}$	0	0	0.09	0.08	0.20	0.15	0.24	0.25
$f_{5/2}$	0.77	0.77	0.34	0.34	0.07	0.07	0.09	0.09
$p_{1/2}$	1.12	1.12	0.76	0.73	0.55	0.45	0.98	0.80
$f_{7/2}$	>2.6	>2.6	>2.7	>2.7	>3.1	>2.8	>3.4	>3.1

ferences in the angular distributions are also observed in (p,d) reactions.[14]

A second indication of the J values of nuclear levels may be obtained by comparing (d,p) and (d,t) cross sections for exciting the level in question. The (d,t) cross section for exciting a nuclear level is proportional to the "fullness" of the single-particle state to which the nuclear level belongs, whereas the (d,p) cross section is proportional to the "emptiness" of the single-particle state.[6] Hence the ratio of (d,p) to (d,t) cross sections is proportional to the emptiness of a shell-model state divided by its fullness. Levels belonging to shell-model states which are not equally full will have different $(d,p)/(d,t)$ cross-section ratios.

In the nickel isotopes, this ratio technique may be applied to the $f_{7/2}$ and $f_{5/2}$ and the $p_{3/2}$ and $p_{1/2}$ levels. The $f_{7/2}$ state should be full while the $f_{5/2}$ state is just beginning to fill, so that f levels having very small $(d,p)/(d,t)$ cross section ratios may be assigned as $f_{7/2}$, and levels with relatively large cross-section ratios, as $f_{5/2}$.

Likewise, the $p_{3/2}$ state is fuller than the $p_{1/2}$ state, because it is more deeply bound, so that a significant difference in the cross-section ratios is expected. Actually, the ratio of spectroscopic factors (see below) should be used, since in this ratio the Q dependence of the single-particle cross section has been removed. The ratios of spectroscopic factors observed in (d,p) and (d,t) reactions are presented in Table VI for all the observed p levels.

As the table indicates, the values of $S(d,p)/S(d,t)$ correctly predict the total angular momentum for all levels where J is known from direct measurements.[15,16] It has been noted, however, that the method seems to fail for a pair of p levels in Fe^{55}. The levels have the same ratio of spectroscopic factors,[2] so that the predicted spins of the levels should be the same, whereas direct measurements assign a different J value to each level.[17]

The ratio method also seems to be unreliable for levels which are very weakly excited. The ratios of Table VI corresponding to levels with relatively small (d,p) and/or (d,t) cross sections (less than 0.05 mb/sr) are enclosed in parentheses. Values of these ratios for the weakly excited levels seem to fluctuate more from level to level and are smaller than corresponding ratios of the more strongly excited levels. The behavior might of explained by two-step excitations or by a "compound nucleus" contribution which are not negligible for levels whose direct reaction cross sections are very small. Nevertheless, the ratio method seems quite reliable for the major levels. According to Table VI, this method suggests J assignments of $\frac{3}{2}$ for the 1.11- and 1.17-MeV levels of Ni^{61}. These assignments are also suggested by the shape of the (d,p) angular distribution at large scattering angles.[18]

Column (3) of Tables I–IV lists the angular momentum assignments used in the present paper. Since the $p_{1/2}$ single-particle state is expected to be at a higher excitation energy than the $p_{3/2}$ state, p levels with unknown J which are far from the ground state are tentatively assigned a J value of $\frac{1}{2}$ unless the total angular momentum is indicated by the ratio method to be $\frac{3}{2}$. Incorrect assignments of l, and consequently S' to experimental angular distributions are possible where states of different l are not resolved. We have tried to minimize such errors by matching the DWBA predictions to experimental data at the stripping peak only. Here contributions from other l transfers will be relatively weak and hence produce the smallest error in S' for the main component of the group. Doubtful and tentative assignments are bracketed in the tables. For a few states no satisfactory fits were found and no assignments were made.

V. DETERMINATION OF S

Values of the spectroscopic factor S are determined from the cross sections of nuclear levels by the relation

$$\frac{d\sigma}{d\Omega}=\frac{2S_0+1}{2S_i+1}\sigma_{s.p.}S=\tfrac{2}{3}(t\sigma_{\mathrm{JULIE}})S' \qquad (2)$$

where $d\sigma/d\Omega$ is the experimental absolute cross section, S_0 the spin of the outgoing triton, and S_i the spin of the incoming deuteron in the reaction. $\sigma_{s.p}=t\sigma_{\mathrm{JULIE}}$ is

[14] R. Sherr, E. Rost, and M. E. Rickey, Phys. Rev. Letters **12**, 420 (1964).
[15] G. A. Bartholomew and M. R. Gunye, Bull. Am. Phys. Soc. **8**, 523 (1963).
[16] R. E. Cote, H. E. Jackson, L. L. Lee, Jr., and J. P. Schiffer, Phys. Rev. **135**, B52 (1964).
[17] D. S. Gemmell, L. L. Lee, Jr., A. Marinov, and J. P. Schiffer, Bull. Am. Phys. Soc. **8**, 523 (1963).
[18] (d,p) reactions at 12 MeV recorded at Aldermaston (Ref. 2) give cross-section ratios between 102.5° and 132.5° (lab angles) of 1.56±0.24 (GS, $p_{3/2}$), 1.76±0.48 (1.11 MeV), 1.64±0.45 (1.17 MeV) and 4.28±0.81 (0.29, $p_{1/2}$).

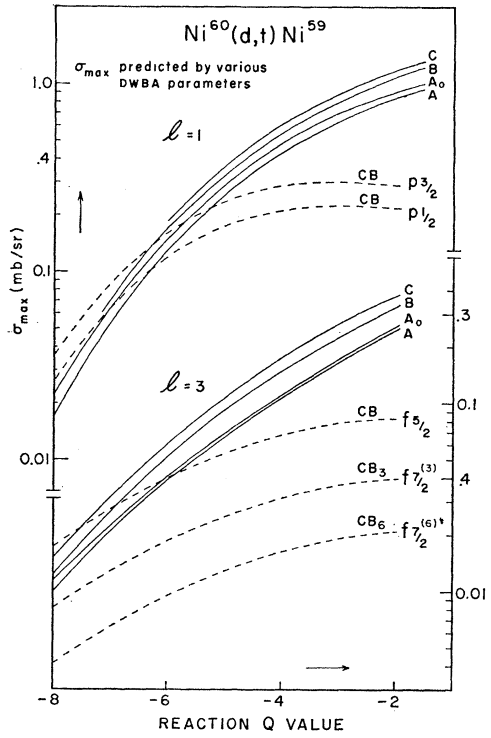

FIG. 11. Q dependence of various theoretical predictions for the differential cross sections at the stripping peak nearest 30° (σ_{JULIE}). Solid lines refer to SE-type calculations for triton parameters A, B, C as explained in Table V. All predictions employ an integration cutoff at 5.5 F except curves A_0, for which no cutoff was used. The dashed curves refer to CB predictions, which depend on l as well as j. Symbols CB_3 and CB_6 are explained in the text.

a single-particle cross section calculated by DWBA methods.[19] As noted in Sec. IV, both the "separation energy" and the "constant binding energy" DWBA calculations were performed. The "constant binding energy" calculations predicted a weaker Q dependence of the cross section than the "separation energy" calculations (~40% change per MeV for the magnitude of $\sigma_{s.p.}$ versus 80%), so that different spectroscopic factors are predicted by the two calculations for a given cross section. Values of absolute cross sections of the stripping peak (near 30°) for the levels in Ni^{57}, Ni^{59}, Ni^{61}, and Ni^{63} are listed in column (4) of Tables I–IV. The corresponding values of S' are listed, for the "separation energy" and "constant binding energy" calculations, in columns (5) and (6) of tables, respectively. As the tables indicate, the values of spectroscopic factors determined by the two methods differ, for some levels, by as much as a factor of 4. However, the most strongly excited levels belonging to a single-quasiparticle state often are located near the position of that single-quasiparticle state, and for these levels, spectroscopic factors derived from the two DWBA calculations are in close agreement.

DWBA calculations were made only for the $Ni^{60}(d,t)$-Ni^{59} reactions, but were used to find spectroscopic factors in all the isotopes studied; that is, changes in the magnitude of $\sigma_{s.p.}$ with change in the neutron excess are ignored. It is felt that the errors incurred by this procedure are smaller than the other uncertainties involved in the determination of the renormalized magnitude of the spectroscopic factors (see Sec. VI below). Furthermore, deuteron-optical-model parameters were not available for most of the other isotopes.

As was mentioned above, various choices of reasonable parameters for the distorted deuteron and triton waves and the integration cutoff had only minor effects on the predicted angular distributions. Even the assumption of constant binding energy (CB) for a given J in the calculation of the neutron form factor did not produce any markedly superior or inferior fits to observed angular distributions. However, the theoretical results varied considerably as to the predicted absolute cross sections, and the resulting magnitudes of S'. Figure 11 shows predicted cross sections for the $l=1$ and $l=3$ maxima near 30°, which can be most easily observed. For the conventional (SE) calculations (solid lines) we see an essentially identical Q-value dependence; but absolute magnitudes can differ by ±30% from the average, depending on the choice of cutoff and triton parameters. This type of uncertainty in S' can very easily be taken care of, together with experimental scale errors, by the type of renormalization described below.

For the derivation of S' as tabulated in Tables I to IV, we arbitrarily selected the deepest triton potential (triton A) as the most realistic, and took a lower integration cutoff of 5.5 F because it produced somewhat better agreement with experimental (d,t) cross sections.

The dotted lines in Fig. 11 show the Q-value dependence of the peak cross sections predicted by the CB calculations (for triton A parameters and a lower cutoff at 5.5 F). The Q dependence differs quite markedly from the conventional (SE) calculations. The neutron binding energies used in all CB calculations were 11.5 MeV for the $2p_{3/2}$ states, 12.1 MeV for the $1f_{5/2}$ states, 12.5 MeV for the $2p_{1/2}$ states, 14.9 MeV for the $1g_{9/2}$ states and 15.1 or 18.1 MeV for the $1f_{7/2}$ states. Where possible the spacing of these states was taken from the Ni^{57} single-particle energies, as reported in this paper. Energies for the $g_{9/2}$ and $f_{7/2}$ states were obtained by extrapolation from quasiparticle energies of adjacent nuclei. The depth of the neutron well was adjusted to give, on the average, the correct asymptotic wave functions for neutrons in Ni^{60}. It is, therefore, somewhat too shallow (by 0.5 MeV) for Ni^{58} too and deep for Ni^{62} and Ni^{64} (by 0.8 and 1.7 MeV, respectively). If the asymptotic behavior of the neutron wave function is important one might, therefore, expect absolute spectroscopic factors S' (for CB calculations) which are

[19] The factor t includes factors peculiar to the (d,t) reaction such as number of neutrons transferable, d,t wave function overlap, etc., and is not included in program JULIE. The best recent estimates give $t \approx 5$ [R. Bassel (private communication)].

TABLE VIII. Renormalized values of V_j^2.

(1)	(2a)	(2b)	(3a)	(3b)	(4a)	(4b)	(5a)	(5b)	(5c)
	$V^2(p_{3/2})$		$V^2(p_{1/2})$		$V^2(f_{5/2})$			$V^2(f_{7/2})$	
Isotope	SE	CB	SE	CB	SE	CB	SE	CB_6	CB_3
Ni^{58}	0.27	0.27	0.12	0.13	0.12	0.11	>0.35	>1.18	>0.59
Ni^{60}	0.58	0.56	0.30	0.33	0.18	0.18	>0.90	>2.85	>1.42
Ni^{62}	0.64	0.58	0.46	0.48	0.33	0.33	>0.53	>1.43	>0.71
Ni^{64}	0.71	0.64	0.63	0.62	0.50	0.52	>0.33	>0.71	>0.35

consistently too large for $Ni^{62}(d,t)$ and $Ni^{64}(d,t)$. The Q dependence of the predicted cross sections does not seem to be strongly affected by moderate changes in the over-all well depth. This is illustrated in Fig. 11 for the $f_{7/2}(\Delta J=3+\frac{1}{2})$ transitions for which we show a calculation for $E_B=-15.1$ MeV (CB_3) (close to the estimated experimental value) and for $E_B=-18.1$ MeV (CB_6). The latter value as arrived at from the known binding of the $f_{5/2}$ particle by postulating a 6-MeV splitting due to the spin-orbit interaction for $l=3$ states.

The use of experimental energies for the neutron form factor is somewhat arbitrary. Other investigators[14] have used the neutron well from the simple j-j shell model. The choice of the well depths does effect the absolute value of the predicted cross sections, but the magnitudes of the relative (or the normalized) spectroscopic factors seem to depend mainly on the splitting of the $l+\frac{1}{2}$ and $l-\frac{1}{2}$ levels. For instance, the predicted transition probabilities to $f_{7/2}$ states are consistently larger by a factor of 2 if the $f_{7/2}-f_{5/2}$ splitting is assumed to be 3 MeV (CB_3) instead of 6 MeV (CB_6) (see Fig. 11).

Apart from the continuing uncertainty as to the most realistic representation of the neutron form factor,[5,20] some spectroscopic factors given could be in error because of incorrect l assignments or levels missed. The CB calculations yielded absolute, unnormalized magnitudes of S' which are too large for Ni^{62} and Ni^{64}. This was expected because the ground-state Q values for (d,t) reactions change noticeably. For Ni^{58}, Ni^{60}, Ni^{61}, Ni^{62}, and Ni^{64} they are -5.676, -5.136, -1.513, -4.366, and -3.400 MeV, respectively.

VI. LOCATION AND FULLNESS OF SINGLE-PARTICLE STATES

The energies E_j of the single-quasiparticle states were found from the data of Tables I–IV. The values of E_j were taken as the "center of gravity" of the observed nuclear levels, as explained in the introduction. The results for the location of the single-quasiparticle states derived from "separation energy" and "constant binding energy" calculations are presented in Table VII, columns (2a)–(5a) and (2b)–(5b), respectively. Because observed nuclear levels belonging to a given single-particle state generally are not spread over a large energy range, the Q dependence of the DWBA calculations has little effect on E_j, and essentially the same results are determined from the "separation energy" and "constant binding energy" calculations. These energies are in fair agreement with the energies found from (d,p) reactions,[2] but tend to be somewhat lower. This is expected, since some levels observed at relatively high excitation energies in the (d,p) reactions have too small a cross section to be observed in the corresponding (d,t) reactions.

If no important levels are missed, the "fullness" of the single-quasiparticle states can also be determined. The fractional "fullness" of the state j is found[6] as the sum $[\sum S_j(d,t)]/(2j+1)$ of the spectroscopic factors of the nuclear levels belonging to the single-particle state j. This sum is equivalent to the parameter V_j^2 of pairing theory.[21]

The values of V_j^2 determined from the present experiment presented in Table VIII have been renormalized. In order to correct for scale errors in the absolute magnitude of both the experimental cross sections and the DWBA calculations, we required that for each isotope the filling shell be populated with the proper number of neutrons, and introduced a separate correction factor c for each isotope, where c is defined by

$$\frac{1}{2j+1}c\sum_i S'^i_j(d,t)=V_j^2. \tag{3}$$

Since $(2j+1)V_j^2$ gives the number of neutrons in the state j, we required

$$\sum_j c\sum_i S'^i_j(d,t)=n, \tag{4}$$

where for the isotope in question, n is the known number of neutrons in the shells being filled. Clearly, Eq. (4) must hold if the numbers V_j^2 are to have their intended meaning. The results of this method are presented for both the "separation energy" and "constant binding energy" DWBA calculations in columns (2a)-(5a) and (2b)-(5b) of Table VIII. The renormalization factors c needed for "constant binding energy" (and "separation energy") calculations, were 1.09 (1.02), 0.87 (0.94), 0.61 (0.76), and 0.54 (0.90), for the Ni^{58}, Ni^{60}, Ni^{62}, and Ni^{64} reactions, respectively. Most of these factors c are different from unity, especially for the CB calculations. If we insist that all large experimental errors are

[20] J. L. Yntema and G. R. Satchler, Phys. Rev. 134, B976 (1964).

[21] L. S. Kisslinger and R. A. Sorenson, Kgl. Danske Videnskab. Selskab, Mat. Fys. Medd. 32, No. 9 (1960).

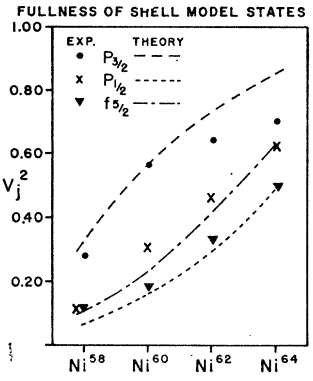

FIG. 12. "Renormalized" spectroscopic factors (V_j^2) of the single-quasiparticle states of the nuclei investigated are compared with theoretical predictions. Figure 11 shows experimental values for V_j^2 extracted with the help of conventional (SE) neutron-form-factor calculations. [Table VIII shows experimental values for V_j^2 obtained under the constant binding energy (CB) assumption for the neutron form factor.]

scale errors and do not exceed $\pm 20\%$, we must conclude that the CB calculations gave only fair predictions for the single-particle cross sections, and that the unnormalized spectroscopic factors may easily be in error by 50% or more.

Our renormalization will take care of experimental scale errors (e.g., uncertain target thickness) and uncertain theoretical factors such as the strength of the interaction, d,t overlap and, partially, the neutron well depth. In general, one would feel more confident with a calculation where the correction factors c change least from isotope to isotope. However, some changes in c must be expected here since Ni^{60} calculations were used for all Ni isotopes, which ought to be described by optical wells of somewhat different sizes and depths.

As Table VIII indicates, the results of the two determinations of V_j^2 generally agree with each other except for the $f_{7/2}$ case, where the values derived from the "separation energy" calculations differ from those of the "constant binding energy" calculations by about a factor of 2. Our best estimates (SE) for V_j^2 are compared with the pairing theory predictions in Fig. 12. The predictions are based on the pairing theory parameters of Ref. 21, except that the values of the single-particle energies, in the absence of pairing interactions, are taken from Table VII as the energies E_j for Ni^{57}.

The values of V_j^2 exhibit the expected trend. As neutrons are added to the shell, the fullness of the low-lying states increases. The $p_{3/2}$ state, most deeply bound, fills most rapidly, followed by the $f_{5/2}$ and $p_{1/2}$ states; but the latter fills faster than expected. The $g_{9/2}$ state seems to be just starting to fill in the heavier nickel isotopes; very weak $l=4$ transitions are observed in the reactions $Ni^{62}(d,t)Ni^{61}$ and $Ni^{64}(d,t)Ni^{63}$.

Another estimate of the fullness of the $f_{5/2}$ subshell can be obtained by comparing values of $\sum S(d,t)$ for the $f_{5/2}$ state with similar values for the $f_{7/2}$ state. The $f_{7/2}$ subshell is practically full in the nickel isotopes; hence if $\sum S$ corresponding to the total excitation strength of the $f_{7/2}$ state is determined, the ratio of $\sum S$ for the $f_{5/2}$ state to that for the $f_{7/2}$ state should equal $V^2(f_{5/2})\times 6/8$. This method eliminates the need for the normalization procedure above.

TABLE IX. Values of $V^2(f_{5/2})$ by comparison with $V^2(f_{7/2})$.

(1)	(2a)	(2b)		(3)
	$V^2(f_{5/2})$ by comparison with $V^2(f_{7/2})$			$V^2(f_{5/2})$ best estimate
Isotope	SE	CB_6	CB_3	(Table VIII)
Ni^{58}	$\lesssim 0.22$	$\lesssim 0.06$	$\lesssim 0.12$	0.12
Ni^{60}	$\lesssim 0.16$	$\lesssim 0.05$	$\lesssim 0.10$	0.18
Ni^{62}	$\lesssim 0.53$	$\lesssim 0.20$	$\lesssim 0.40$	0.33
Ni^{64}	<1.35	<0.65	<1.30	0.51

To determine the proper value of $\sum S$ for the $f_{7/2}$ state, the measured values have been corrected for the fact that the total excitation strength of the $f_{7/2}$ state is divided by isotopic-spin splitting into two groups of nuclear levels, only the lower of which lies within the energy region of the present experiment. The fraction of the total $f_{7/2}$ strength contained in the lower group of nuclear levels is theoretically predictable[22] and provides the correction factor applied to the values of $\sum S$ found from the observed levels. The presented values of $V^2(f_{5/2})$ as determined from this procedure would have to be reduced if not all the $f_{7/2}$ levels in the lower group were observed. Unobserved $f_{7/2}$ levels may possibly exist in all the nuclei studied, although an analysis of the spectra indicates that major $f_{7/2}$ levels were probably missed only in the $Ni^{64}(d,t)Ni^{63}$ reactions, where triton levels from target impurities hindered the investigation of the high-energy region. Accordingly, the values of $V^2(f_{5/2})$ determined by this method should be considered as upper limits, particularly in the Ni^{64} case. The values are presented in Table IX and compared with similar values from the best estimates of V_j^2. As Table IX indicates, the upper limits of $V^2(f_{5/2})$ are in fair agreement with the "best estimates" when the "separation energy" calculations are used to determine $\sum S$, but in poorer agreement when the "constant binding energy" calculations are used.

TABLE X. Results of the $Ni^{61}(d,t)Ni^{60}$ reactions.

(1) Excitation energy (MeV)	(2) l	(3) J	(4) $(d\sigma/d\omega)_{max}$	(5) S' SE
0	1	0^+	1.45	0.46
1.33	1	2^+	1.36	0.62
2.17	3	$2^{(+)}$	0.09	0.22
2.29	1	(0^+)	0.17	0.11
2.52	3	4^+	0.15	0.44
2.63	3		0.28	0.86
2.81	1		0.10	0.08
3.14	1	$2^{(+)}$	0.59	0.58
3.26	1		0.33	0.34
3.40	1		0.43	0.49

[22] J. B. French and M. H. MacFarlane, Nucl. Phys. **26**, 168 (1961).

VII. THE $Ni^{61}(d,t)Ni^{60}$ REACTION

The results of the investigation of Ni^{60} by (d,t) reactions are presented in Table X. Column (1) of this table lists the energies, column (2) lists l, column (3) the total angular momentum, and column (4) the cross sections of the observed levels. Angular distributions of the observed levels are shown in Fig. 7. Because of uncertainties in the j values of several strong levels, the spectroscopic factors S' extracted from the data [column (5)] are not discussed in terms of shell-model theory. The j values listed are taken from the Nuclear Data Tables. All are consistent with our pickup data. The parities of all levels observed are positive.

VIII. SUMMARY AND CONCLUSIONS

The work presented in this paper was initiated as a supplement for the spectroscopic work on the Ni^{59}, Ni^{61}, and Ni^{63} isotopes presented in Refs. 2 and 3. In addition spectroscopic information on Ni^{57} was sought. In good agreement with a previous (p,d) experiment,[23] only four levels were seen in Ni^{57}, in spite of our improved energy resolution. If the state near 0.77 MeV is a doublet as suggested in Ref. 23, its spacing must be less than 50 keV.

For Ni^{59}, Ni^{61}, and Ni^{63} a large number of l and j assignments, given in Refs. 1 and 2, was confirmed, and a few new assignments were made. As shown in Tables I–IV several $f_{7/2}$ states are found below 4-MeV excitation for all Ni isotopes. Some of these states (weakly) excited by $l=3$ (d,p) transitions had previously been assumed to be $f_{5/2}$ (Refs. 1–2). However, their strong excitation by (d,t) reactions indicates that they are $f_{7/2}$ states. This is an interesting indication that in the light Ni isotopes the $f_{7/2}$ shell is not completely filled.

The new j assignments affect the values of E_j and U_j^2 in Refs. 1 and 2 in a systematic fashion, since previously all higher lying p and f levels were assumed to have total angular momentum $\frac{1}{2}$ and $\frac{5}{2}$, respectively. Values for the $f_{5/2}$ quasiparticle energies will have to be lowered, those for $p_{3/2}$ have to be raised. This change much improves the agreement with our E_j values from the (d,t) experiment (Table VII). The agreement of the calculated fullnesses from (d,p) results for the $p_{3/2}$, $f_{5/2}$, and $p_{1/2}$ states again is good, once the j values and normalization used in Refs. 1 and 2 are brought up to date.[24]

It should be noted that the $p_{1/2}$ state appears much fuller than predicted by shell-model theory (Fig. 12). This deviation may just reflect the various approximations made in our DWBA calculations, but it may also be significant.

In the latter case, one explanation might be that some $l=1$ transitions seen in the experiments no longer lead to states which are well described as single-quasiparticle states.

The combination of (d,p) and (d,t) experiments usually allows a safe determination of l and j for all reasonably strongly excited states. While the majority of our j assignments stems from a comparison of (d,t) and (d,p) cross sections, a number of j values for p states could be unambiguously assigned by a comparison of large angular distributions (see Figs. 5 and 10 and Ref. 13). For f states the identification of the correct j value from the (d,t) angular distribution seems also possible, but generally more accurate data are needed. Differences for $f_{5/2}$ and $f_{7/2}$ angular distributions occur at forward angles, but are not as clear as those for $p_{3/2}$ and $p_{1/2}$ states (compare Figs. 6 and 5), and the observed shift in position and shape of the forward maximum is partly (although not entirely) due to the Q value differences for the $f_{5/2}$ and $f_{7/2}$ transitions. There is evidence that spin-dependent DWBA calculations can correctly predict the empirically observed j dependence in stripping and pickup reactions.[25] Such calculations will generally yield better quantitative agreement with large angle experimental cross sections than calculations in which $\mathbf{l}\cdot\mathbf{s}$ terms were neglected. DWBA calculations for the present (d,t) work, which were made without spin-orbit terms, usually differed substantially from the data at angles larger than 70°. This, of course, is to be expected whenever the j effect is as strong as shown in Figs. 5 and 10.

As mentioned above the neutron form factor used in our calculations, whether of the standard type (SE) or kept constant for a given j (CB) had little effect on the predicted angular distributions. However, there was a very noticeable difference in the predicted Q-value dependence of the pickup cross sections (Fig. 11), and as a consequence, in the extracted spectroscopic factors. It appears that our (d,t) experiment is a useful test case for the two approaches since both calculations turn out more Q sensitive than usual. Even so the relatively small energy spread in the observed $p_{3/2}$, $f_{5/2}$, and $p_{1/2}$ states obscures any difference in the two approaches for these levels. The $f_{7/2}$ spectroscopic factors, however, do differ very significantly, as can be seen in Tables I–IV. We know that we do not observe all $f_{7/2}$ states, because of the high negative Q values for some $f_{7/2}$ levels; hence all observed fullnesses (Table VIII) for the $f_{7/2}$ level are lower limits, which must always be well below 1.00. It is seen that the standard calculations (SE) meet this condition, whether the data are renormalized or not. CB calculations ($CB=CB_6$), however, yield fullnesses well over 100% (even after renormalization) for any reasonable $f_{5/2}$-$f_{7/2}$ splitting. In order to check the dependence of this conclusion on the assumed spin-orbit splitting we calculated fullnesses for an assumed $f_{5/2}$-$f_{7/2}$ splitting of 3 MeV (listed under CB_3) which must certainly be considered as a lower limit for the splitting. Even in this case the predicted $f_{7/2}$ fullnesses are too

[23] J. C. Legg and E. Rost, Phys. Rev. **134**, B753 (1964).
[24] R. H. Fulmer, Ph.D. thesis, Pittsburgh, 1964 (unpublished).
[25] L. L. Lee, Jr., A. Marinov, C. Mayer-Boricke, J. P. Schiffer, R. H. Bassel, R. M. Drisko, and G. R. Satchler, Phys. Rev. Letters **14**, 261 (1965).

high, at least for Ni^{60}. It seems, therefore, that in calculations for the Ni(d,t) reactions the correct asymptotic behaviour of the neutron form factor is important, and CB calculations give results less consistent than the standard (separation energy) methods.

ACKNOWLEDGMENTS

The authors are indebted to Professor R. M. Drisko for his advice and help in performing the DWBA calculations and to Professor B. L. Cohen and Professor R. M. Drisko for helpful discussions during the course of this work. Thanks are also due to Dr. R. K. Jolly for assistance in the accumulation of data and to Dr. J. K. Dickens for providing the Ni^{64} target on loan. The DWBA calculations reported in this article were performed at the University of Pittsburgh computation center, which is partially supported by the National Science Foundation under Grant No. B-11309.

PHYSICAL REVIEW VOLUME 139, NUMBER 3B 9 AUGUST 1965

α Particles from the Triton Bombardment of Li^7, C^{12}, and O^{16}†

F. AJZENBERG-SELOVE AND J. W. WATSON
Haverford College, Haverford, Pennsylvania

AND

R. MIDDLETON
University of Pennsylvania, Philadelphia, Pennsylvania

(Received 22 March 1965)

A Li^7 oxide layer deposited on a carbon foil has been bombarded by 13-MeV tritons from the Aldermaston tandem. The spectra of α particles emitted at 24 angles relative to the incident beam (5° to 175°) have been determined with the Aldermaston multigap spectrograph, using nuclear plates as detectors. The first excited state of He^6 is found to have an excitation energy of 1.797 ± 0.025 MeV and a width of 113 ± 20 keV. No other excited states of He^6 below an excitation energy of 12 MeV have been observed, for $\theta=5°$ to 35°. Angular distributions of α particles have been determined to the following states: $E_x=0$ and 1.80 MeV in He^6; $E_x=0$, 5.28+5.31, and 6.33 MeV in N^{15}; $E_x=0$, 2.14, 4.46, and 5.03 MeV in B^{11}. The angular distributions show strong direct-interaction features.

INTRODUCTION

THE only exoergic reaction leading to He^6 is the $Li^7(t,\alpha)He^6$ reaction with a Q value of 9.833 MeV.[1] It is therefore not surprising that most of the known information on the structure of He^6 has been derived from work with this reaction. K. W. Allen *et al.*[2–4] have observed two excited states of He^6 with $E_x=1.71\pm0.01$ MeV ($\Gamma\lesssim100$ keV) and 3.4 ± 0.2 MeV ($\Gamma<300$ keV). These experiments used low-energy tritons ($E_t<1$ MeV), and a proportional-counter technique. The α-particle group attributed to the 3.4-MeV state[4] was observed at $\theta=131°$ at $E_t=0.24$ MeV, and at $\theta=90°$ at $E_t=0.71$ and 0.90 MeV. Evidence has also been reported[5] for one or more states at $E_x=9.3\pm0.7$ MeV and possibly for a state at $E_x=6\pm0.9$ MeV. The summed proton spectrum from the $Li^7(p,2p)He^6$ reaction suggests[1] an excited state of He^6 with $E_x\sim15$ MeV and $J=1^-$ or 2^-. It appears fair to say that only the existence of an excited state with $E_x\sim1.7$ MeV has been established with any certainty.

While there is no question of the existence of the 1.7-MeV state, its parameters and decay modes are only poorly established. Its angular momentum and parity are probably[6,7] 2^+, but there has been conflicting evidence on its width and on its decay modes. There have been reports that the 1.7-MeV state decays by γ emission.[8,9] On the other hand the absence of He^{6*} recoils,[3] and the fact that the state is broad,[10] suggest that the decay is by particle emission via one or both of the

† The exposure of the plates was carried out at the Atomic Weapons Research Establishment, Aldermaston, England. The remainder of this work was supported by the National Science Foundation.

[1] T. Lauritsen and F. Ajzenberg-Selove, Nucl. Phys. (to be published).
[2] J. T. Dewan, T. P. Pepper, K. W. Allen, and E. Almqvist, Phys. Rev. **86**, 416 (1952).
[3] K. W. Allen, E. Almqvist, J. T. Dewan, and T. P. Pepper, Phys. Rev. **96**, 684 (1954).
[4] K. W. Allen, E. Almqvist, and C. B. Bigham, Proc. Phys. Soc. (London) **75**, 913 (1960).
[5] D. Magnac-Valette and P. Cüer, J. Phys. Radium **17**, 553 (1956); Physica **22**, 1156A (1956).
[6] E. Almqvist, T. P. Pepper, and P. Lorrain, Can. J. Phys. **32**, 621 (1954).
[7] S. H. Levine, R. S. Bender, and J. N. McGruer, Phys. Rev. **97**, 1249 (1955).
[8] E. W. Titterton and T. A. Brinkley, Proc. Phys. Soc. (London) **67**, 469 (1954).
[9] D. Magnac-Valette, R. Seltz, R. Bilwes, and J. Spyns, in *Proceedings of the Conference on Direct Interactions and Nuclear Reaction Mechanisms Padua (1962)*, edited by E. Clementel and C. Villi (Gordon and Breach Publishers Inc., New York, 1963), p. 1088A.
[10] F. Ajzenberg-Selove and R. Middleton, Bull. Am. Phys. Soc. **9**, 391 (1964).